Fault diagnostics and evaluation in cryogenic loading system using optimization algorithm

Ekaterina Ponizovskaya-Devine[1], Dmitry G Luchinsky[2], Anu Kodali[3], Michael Khasin[4], Dogan Timucin[5], Jarred Sass[6], Jose Perotti[7], Barbara Brown[8]

[1,3,4] *SGT, Inc., Greenbelt, MD, 20770, USA*
ekaterina.v.ponizovskayadevine@nasa.gov
anupa.r.bajwa@nasa.gov
michael.khasin@nasa.gov

[2] *Mission Critical Technologies, Inc., El Segundo, CA, 90245, USA*
dmitry.g.luchinsky@nasa.gov

[5] *NASA Ames Research Center, Moffett Field, CA, 94035, USA*
dogan.timucin@nasa.gov

[6,7,8] *Kennedy Space Center, Kennedy Space Center, FL, 32899, USA*
jose.m.perotti@nasa.gov
jared.p.sass@nasa.gov
barbara.l.brown@nasa.gov

Abstract

Physics-based approach to the cryogenic flow health management is presented. It is based on fast and time-accurate physics models of the cryogenic flow in the transfer line. We discuss main features of one of these models – the homogeneous moving front model – and presents results of its validation. The main steps of the approach including fault detection, identification, and evaluation are discussed. A few examples of faults are presented. It is shown that dynamic features of the faults naturally form a number of ambiguity groups. A D-matrix approach to optimized identification of these faults is briefly outlined. An example of discerning and evaluating faults within one ambiguity group using optimization algorithm is considered in more details. An application of this approach to the Integrated Health Management of cryogenic loading is discussed.

1. Introduction

Future of the space exploration requires development of the Integrated Health Management (IHM) of cryogenic systems on the ground and in space (Chato, 2008). Cryogenic propellant loading operations are some of the most complex, critical activities in launch operations (Johnson, Notardonato, Currin, & Orozco-Smith, 2012). Full potential of autonomous intelligent health management of such systems on the ground and in space can be achieved by using fast and time-accurate physics models of the two-phase cryogenic flow.

Predicting the behavior of the two-phase flows is a long standing problem (Prosperetti & Tryggvason, n.d.). To solve this problem we developed a hierarchy of the models of two-phase cryogenic flows (Luchinsky, Smelyanskiy, & Brown, 2014a), verified and validated their performance (Luchinsky, Smelyanskiy, & Brown, 2014b; Hafiychuk et al., 2014, 2015). The models are fast and accurate enough to allow for on-line applications to the cryogenic health management, including on-line solution of the optimization problem.

In this paper we describe the progress in development of such physics based approach to fault isolation and recovery for cryogenic loading operation. We present moving front model of the two-phase cryogenic flow (Zhang & Zhang, 2006; Hafiychuk et al., 2014, 2015) and the results of its validation. Next we discuss the application of this model to the creation and extension of the digital library of faults related to the cryogenic loading operation. We demonstrate that these faults naturally form a number of ambiguity groups with similar dynamic features within each group. We propose to use D-matrix formalism (Sheppard & Simpson, 1996) to enhance identification of the faults with multiple ambiguity groups. To optimize the performance of the D-matrix method we propose to use iDME tool (Singh et al., 2009). The focus of the current paper is on the discussion of the development of on- and off-line optimization tools that can be used to discern and evaluate faults within one of the ambiguity groups. We present the results of numerical test in which one of the faults (valve stack open) was identified within ambiguity group. We use optimization algorithms to discern this fault from other possible faults (another valve stack open and a gas leak). We verified the performance of three optimization algorithms (local unconstrained nonlinear optimization, direct search, and Markov Chain Monte Carlo (MCMC)). We demonstrated that direct search algorithm can correctly identify and evaluate the fault. Finally, we provide the conclusions and discuss future work.

2. MODEL

The homogeneous model of the two-phase flow describes the flow dynamics and thermodynamics in terms of conservation laws for the mass, momentum, and energy

$$\begin{gathered}\rho_{,t} + (\rho u)_{,z} = 0 \\ (\rho u)_{,t} + \left(\rho u^2\right)_{,z} = -p_{,z} - \tfrac{1}{A}(\tau_w l_w)_{2\phi} - \rho g \sin\theta \\ (\rho e)_{,t} + (\rho u h)_{,z} = \tfrac{1}{A}\dot{q}_w l_w\end{gathered}$$

written for the mixture density ρ and enthalpy h

$$\rho = \alpha\rho_v + (1-\alpha)\,\rho_l; \qquad h = x h_v + (1-x)\,h_l$$

and coupled to the equation for the wall temperature

$$\rho_w c_w d_w \frac{\partial T_w}{\partial t} = H_w\,(T - T_w)\,l_i + H_a\,(T_a - T_w)\,l_o. \quad (1)$$

The set of the model equations is closed by adding equation of state to the system

$$\rho_{(g,l)} = \rho_{(g,l)}\left(p, h_{(g,l)}\right). \quad (2)$$

The moving front version of this model (Zhang & Zhang, 2006) allows one to incorporate up to three coexisting states of the fluid (vapor, liquid, and their mixture) within one control volume, therefore, increasing fidelity of the model.

In the particular version of the moving front model developed in (Hafiychuk et al., 2014, 2015) the momentum equation is solved in the quasi-steady approximation, neglecting inertia terms

$$\left(A\rho u^2\right)_{,z} + \frac{1}{A}(\tau_w l_w)_{2\phi} = -p_{,z} - \rho g \sin\theta.$$

In this approach calculations of the mass fluxes is decoupled from the integration of the conservation equations for the mass and energy. The resulting algorithm allows for very fast and time-accurate predictions of the cryogenic two-phase flow in transfer lines. The speed of the calculations can be further improved by using non-conservative linearized version of the mass and energy conservation equations.

2.1. Vapor region

The specific form of the linearized equations depends on the type of the flow. For example, using Taylor expansion for the density in terms of pressure and enthalpy

$$d\rho = \frac{\partial\rho}{\partial p}dp + \frac{\partial\rho}{\partial h}dh$$

we obtain for the pure vapor region the following set of equations

$$\begin{gathered}\tfrac{\partial\rho_g}{\partial p}\tfrac{dp}{dt} + \tfrac{\partial\rho_g}{\partial h_g}\tfrac{dh_g}{dt} = \tfrac{\dot{m}_{in} - \dot{m}_{out}}{\Delta z A} \\ \left(\tfrac{\partial(\rho_g h_g)}{\partial p} - 1\right)\tfrac{dp}{dt} + \tfrac{\partial(\rho_g h_g)}{\partial h_g}\tfrac{dh_g}{dt} = \tfrac{(\dot{m}_g h_g)_{in} - (\dot{m}_g h_g)_{out}}{\Delta z A} \\ + \tfrac{4}{D} H_{wg}\,(T_w - T_g)\end{gathered}$$

For liquid control volume the equations are exactly the same on the substitution of subindex g (for a gas) on subindex l (for a liquid).

2.2. Two-phase region

In the case of the two-phase flow region we have (Zhang & Zhang, 2006; Hafiychuk et al., 2014, 2015)

$$\begin{gathered}\left(\left(\bar{\alpha}\tfrac{\partial\rho_g}{\partial P} + (1-\bar{\alpha})\tfrac{\partial\rho_l}{\partial P}\right) + (\rho_g - \rho_l)\tfrac{d\bar{\alpha}}{dP}\right)\tfrac{dP}{dt} \\ + \tfrac{(\rho_g - \rho_l)}{(h_g - h_l)}\tfrac{d\bar{\alpha}}{dx_2}\tfrac{dh}{dt} = \tfrac{1}{V}\left(\dot{m}_{in} - \dot{m}_{out}\right)\end{gathered}$$

$$\begin{gathered}\left(\left(\bar{\alpha}\tfrac{\partial\rho_g h_g}{\partial p} + (1-\bar{\alpha})\tfrac{\partial\rho_l h_l}{\partial p} - 1\right) + (\rho_g h_g - \rho_l h_l)\tfrac{d\bar{\alpha}}{dp}\right)\tfrac{dp}{dt} \\ + \tfrac{(\rho_g h_g - \rho_l h_l)}{(h_g - h_l)}\tfrac{d\bar{\alpha}}{dx_2}\tfrac{dh}{dt} = \\ \tfrac{1}{V}\left((\dot{m}_{in} h_{in} - \dot{m}_{out} h_{out}) + \Delta z H_{amb} D\,(T_w - T)\right)\end{gathered}$$

where

$$\frac{\partial\bar{\alpha}}{\partial b} = \frac{(b+2)/b^3}{(x_2 - x_1)}\ln\frac{1 + b x_2}{1 + b x_1} - \frac{1}{b^2} - \frac{(1+b)/b^2}{(1 + b x_1)(1 + b x_2)}.$$

Here $x_{1,2}$ are the flow quality on the left (z_1) and right (z_2) boundaries of the two-phase region, $\bar{\gamma}(p, x_2)$ is the averaged void fraction in the two-phase region defined as

$$\bar{\alpha}\,(P, x_2) = \frac{1}{z_2 - z_1}\int_{z_1}^{z_2} dz\alpha.$$

The flow quality is assumed to change linearly with coordinate as follows

$$x\,(z) = x_1 + (x_2 - x_1)\,(z - z_1)\,/\,(z_2 - z_1)$$

and the variable $b(p)$ is defined using correlations (Woldesemayat & Ghajar, 2007)

$$b\left(p\right) = \left(\frac{\rho_l}{\rho_g}\right)^{n_1} \cdot \left(\frac{\mu_g}{\mu_l}\right)^{n_2} - 1 > 0.$$

2.3. Vapor and two-phase region in one control volume

As we mentioned above, to elevate fidelity of the model the mixed control volumes are allowed. Here we consider one example of such control volume filled with vapor and two-phase region. It is assumed that the location of the boundary between two regions $L_2(t)$ is changing with time. In this case we have to solve two sets of two-dimensional equations for each region considered in two previous sections simultaneously with the equation for the moving boundary (Jensen, Jensen, & Tummescheit, 2002).

In the two-phase region the equations take the form

$$\left(\bar{\alpha}\frac{\partial\rho_g}{\partial p} + \left(1-\bar{\alpha}\right)\frac{\partial\rho_l}{\partial p}\right)\frac{dp}{dt} + \left(\rho_g - \rho_l\right) \times \left[\left(\bar{\alpha}-1\right)\frac{d\ln L_2}{dt} + \frac{d\bar{\alpha}}{dt}\right] = \frac{\dot{m}_{in}-\dot{m}_{23}}{V_2}$$

$$\left[\bar{\alpha}\frac{\partial(\rho_g h_g)}{\partial o} + \left(1-\bar{\alpha}\right)\frac{\partial(\rho_l h_l)}{\partial p} - 1\right]\frac{dp}{dt} + \left(\rho_g h_g - \rho_l h_l\right) \times \left[\left(\bar{\alpha}-1\right)\frac{d\ln L_2}{dt} + \frac{d\bar{\alpha}}{dt}\right] = \frac{\dot{m}_{in}h_{in}-\dot{m}_{23}h_g}{V_2} + \frac{4}{D}H_{wf}\left(T_{w2}-T_2\right)$$

and for the vapor region we have

$$\frac{\partial\rho_3}{\partial p}\frac{dp}{dt} + \frac{\partial\rho_3}{\partial h_3}\frac{dh_3}{dt} + \left(\rho_3-\rho_g\right)\frac{d\ln L_3}{dt} = \frac{\dot{m}_{23}-\dot{m}_{out}}{V_3}$$

$$\left(\frac{\partial(\rho_3 h_3)}{\partial p} - 1\right)\frac{dp}{dt} + \frac{\partial(\rho_3 h_3)}{\partial h_3}\frac{dh_3}{dt} + \left(\rho_3 h_3 - \rho_g h_g\right) \times \frac{d\ln L_3}{dt} = \frac{\dot{m}_{23}h_g - \dot{m}_{out}h_{out}}{V_3} + \frac{4}{D}H_{wg}\left(T_{w3}-T_3\right).$$

These four equations can be solved simultaneously for pressure, enthalpies, and location of the boundary once we assume that the pressure is the same in both regions. We can further speed up calculations if we consider liquid phase to be at saturated conditions in the two-phase region. Similarly, the pressure and enthalpy for the mixture and pure phases can be found in all other cases (Hafiychuk et al., 2014; Jensen et al., 2002).

Once pressure and enthalpies are found one can calculate mass fluxes between the volumes.

3. ALGORITHM

The algorithm is straightforward and consists of two steps. At the first step of the algorithm mass and energy conservation equations are solved for all control volumes once initial conditions for the mass fluxes are provided.

For example for the control volume filled with vapor explicit Euler scheme can be used to advance solution in one time step

$$\begin{bmatrix} b_{11} & b_{12} \\ b_{21} & b_{22} \end{bmatrix} \begin{bmatrix} dp_L \\ dh_{g,L} \end{bmatrix} = \begin{bmatrix} f_1 \\ f_2 \end{bmatrix} dt. \quad (3)$$

The matrix and vector coefficients in Eq. (3) are given by the following equations

$$b_{11,L} = \frac{\partial\rho_{g,L}}{\partial p_L}$$
$$b_{12,L} = \frac{\partial\rho_{g,L}}{\partial h_{g,L}}$$
$$b_{21,L} = \left(\frac{\partial(\rho_g h_g)_L}{\partial p_L} - 1\right)$$
$$b_{22,L} = \frac{\partial(\rho_g h_g)_L}{\partial h_{g,L}}$$
$$f_{2,L} = \frac{(\dot{m}_g h_g)_j - (\dot{m}_g h_g)_{j+1}}{V_L} + \frac{4}{D_L}H_{wg,L}\left(T_{w,L}-T_{g,L}\right)$$
$$f_{1,L} = \frac{\dot{m}_j - \dot{m}_{j+1}}{V_L}.$$

The node notation convention is shown in Fig. 1. Similar equations hold for all other types of control volumes.

At the second step of the algorithm, the momentum equation is solved as follows

$$\frac{\dot{m}_j^2}{A_n^2}\left[\frac{1}{\rho_n}\left(f_n\frac{L_n}{D_n} + \sum K_n\right) + \left(\frac{x^2}{\gamma\rho_g} + \frac{(1-x)^2}{(1-\gamma)\rho_l}\right)_n\right] = -\Delta p_j - \Delta z_j \rho_j g \sin\theta. \quad (4)$$

This equation is applicable when pipe diameters on the both sides of the junction are the same. The subindex n for frictional factor f and minor losses K refers to the control volume on the left or right hand side of the junction.

The stability of this approximation (Thome, 2006) was enforced by the donor-like formulation of the frictional losses for the mass fluxes written in (2) in the following form

$$\left(A\rho u^2\right)\Big|_{z_1}^{z_2} = \frac{\dot{m}_j^2}{2A_n^2}\left(\frac{x^2}{\gamma\rho_g} + \frac{(1-x)^2}{(1-\gamma)\rho_l}\right)\Bigg|_{z_1}^{z_2}.$$

The donor-like formulation assumes that $n = K$ if the right-hand side of the Eq. (4) is positive and $n = L$ otherwise.

4. CORRELATIONS

The thermodynamic and mechanical properties of the two-phase flow within this model are described using the following set of correlations.

The frictional losses coefficients $f_{1,3}$ in Eq(5) were calculated

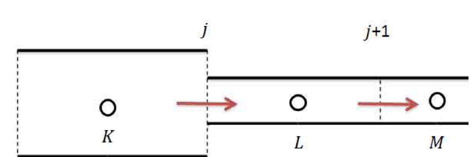

Figure 1. The convention for the nodes and junction notations.

using the Swami-Jain (Thome, 2006) approximation of the Colebrook equation:

$$\frac{1}{\sqrt{f_{1,3}}} = -1.74 \ln\left(\frac{d_r}{3.7D} + \frac{1.26}{\mathrm{Re}_{1,3}\sqrt{f_{1,3}}}\right)$$

$$f_{1,3} = 0.25\left(\log\left(\frac{\epsilon}{3.7D}\right) + \frac{5.74}{Re^{0.9}}\right)^{-2}$$

where ϵ is roughness, D - pipe diameter, and Re is the Reynolds number determined by the following relation mass flow rate $Re = \frac{\dot{m}D}{A\mu}$ with $\dot{m}$ being mass flow rate.

For the two-phase flow the frictional loss coefficient was calculated according to the Mueller-Steinhagen and Heck correlation (Thome, 2006) is

$$f_2 = \frac{\bar{\rho}_2 f_1}{\rho_l (x_2 - x_1)} \left[\frac{\beta}{4}x^4 - \frac{3}{4}(1-x)^{4/3}\left[1 + \frac{2}{7}(\beta - 1)(3 + 4x)\right]\right]\Big|_{x_1}^{x_2}.$$

The Dittus-Boelter approximation (Thome, 2006) was used to calculate the heat transfer:

$$H_{wf} = \alpha H_{wg} + (1-\alpha) H_{wl}$$

$$H_{wv,wl} = \left(\frac{\kappa}{D} Nu\right)_{v,l}$$

$$Nu_{l,g} = 0.023 Re_{l,g}^{4/5} Pr_{l,g}^{2/5}.$$

The boiling enhancement factor was introduced the same way as in the Gungor-Winterton (1987) correlation (Thome, 2006)

$$H_2 = \eta H_0 \left\langle (1-\alpha)^{4/5} E \right\rangle$$

where $\eta = Fr^{0.1-2Fr} if Fr < 0.05$ and $\eta = 1 if Fr > 0.05$. Here

$$E(x) = 1 + 3000 Bo^{0.86} + 1.12\left(\frac{x}{1-x}\right)^{0.75}\left(\frac{\rho_l}{\rho_g}\right)^{0.41}$$

is the boiling enhancement factor, $Fr = \left(\frac{\dot{m}}{\rho_l A}\right)\frac{1}{gD}$ is the Froude number, and $Bo = \frac{H_2(T_w - T_f)A}{\dot{m}(h_g - h_l)}$ is the boiling number.

5. VERIFICATION AND VALIDATION

The moving front model was verified for cryogenic applications by comparison of the model performance with the results of simulations using SINDA/FLUINT code (Kashani et al., 2014). It was also validated by comparison with experimental data obtained at NIST (Brennan, Brentari, Smith, & Steward, 1966) and at KSC (Hafiychuk et al., 2015).

An example of the model validation using experimental data obtained at KSC cryogenic testbed is shown in Fig. 2. Model predictions for the temperature and pressure (red lines) during chilldown in transfer line are shown in comparison with experimental data obtained for temperature and pressure (black lines) obtained in the testbed at KSC. It can be seen from the figure that despite the simplifications introduced to speed up integration, the model can reproduce accurately both pressure and temperature variations at different locations along the line.

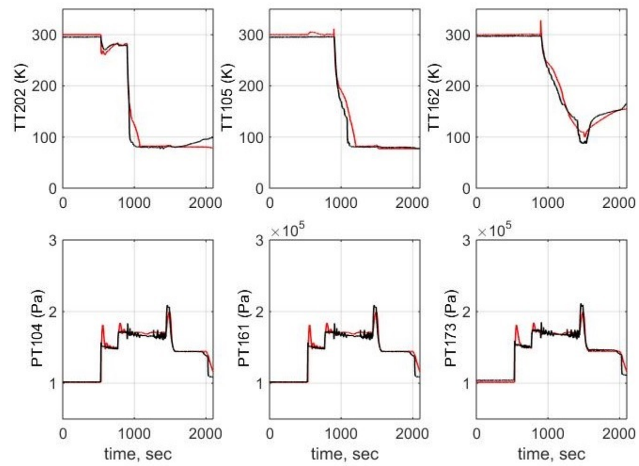

Figure 2. Model predictions (red lines) of the chilldown in cryogenic transfer line are shown in comparison with experimental data (black lines): (top) temperature and (bottom) pressure at three locations alone the line.

The proposed integration scheme is very fast. The 2000 seconds of the real time chilldown in this example were integrated in less than one second of the CPU time on a laptop.

The fast and time-accurate predictions of the cryogenics two-phase flow obtained using this model open a possibility of development of the model-based approach to the integrated health management of cryogenic systems. Below we report on the progress in development of such an approach.

6. PHYSICS BASED APPROACH TO THE FAULT DIAGNOSTICS AND EVALUATION

The online health management of cryogenic systems involves the following set of basic operations: (i) continuous monitoring of the fluid transfer and fault detection; (ii) fault isolation and identification; (iii) fault evaluation. A more advanced IHM can also propose and optimize fault recovery strategies.

In this paper we will discuss briefly how physics-based approach can enhance the performance of an IHM system at every step. We will demonstrate that faults during cryogenic fluid transfer naturally fall within several ambiguity groups. We discuss how physics models can help to improve fault identification using D-matrix formalism. We present an ap-

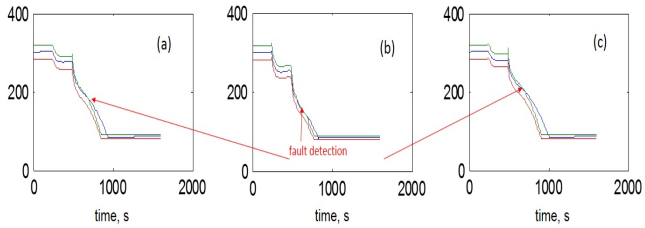

Figure 3. Fault detection in the transfer line when one of the bleed valves is stack closed.

plication of the physics models to discerning and evaluating faults within one ambiguity group.

6.1. Fault detection

An event of fault detection is depicted in the Fig. 3. In this test the transfer line is opened for the fluid flow at around 500 sec and one of the bleed valves in the system is stack closed. This fault causes partial blocking of the upstream flow through the line and chilldown delay. As a result the fluid temperature along the line is higher than in nominal regime. The deviation of the temperature from the nominal dynamics can be detected by several sensors along the line as the crossing of the top margin by the temperature time trace. Once this crossing is observed the system signals fault detection.

Once fault is detected the IHM system should locate and identify it. This task is nontrivial because there are many possible faults in the system, their dynamics is complex, and different faults may often cause similar response of the system.

The model based approach to the IHM allows one to simplify the solution of this problem by building off-line a digital library of such faults and investigating their dynamic features. The dynamic features can be ultimately related to the flow properties via full set of the flow boiling correlations available within the hierarchy of models. This digital library can be extended and improved by continuous experimental validation of some of these faults and by learning model parameters. Here we lay down the foundation of this process and provide some preliminary results of the corresponding analysis.

6.2. Identification

Our example below is focused on the chilldown for two main reasons. Firstly, it is very desirable to detect faults in the cryogenic line at earlier stage before transfer has began. And fault detection at the chilldown stage provides such an opportunity. Secondly, chilldown analysis is very challenging and most of the functional fault models ignore this stage of operation. In this sense the model based approach allows one to fill the corresponding gap in the IHM of cryogenic systems.

The faults in the cryogenic transfer line are most frequently related to the flow blocking or leaks. The flow blocking may have multiple origin including e.g. clogging, valve stack closed, vapor lock.

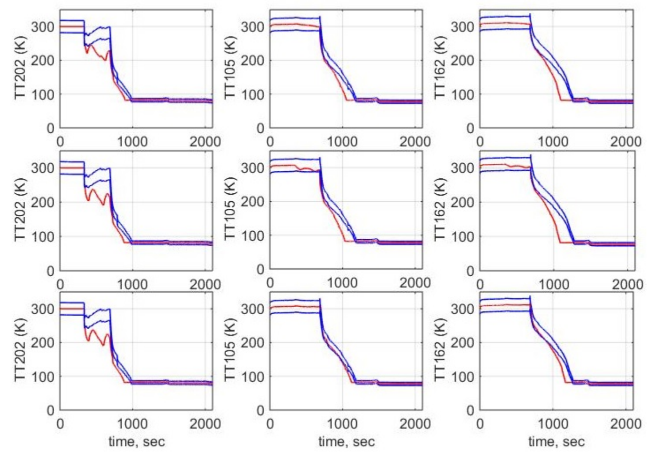

Figure 4. Dynamical features of three faults within one ambiguity group: (top row) bleed valve 1 is stack open, (middle row) bleed valve 2 is stack open, (bottom row) leak in one of the pipes.

Some of these faults have dynamical features similar to those shown in the Fig. 3. These faults correspond to the partial flow blocking and can be detected by several sensors. The faults with similar dynamical features that can not be easily identified are combined in so-called ambiguity groups. The numerical analysis reveals several such ambiguity groups for the faults in cryogenic flow. Identifying faults with similar dynamic features within one ambiguity group is a challenging problem.

Example of another ambiguity group is shown in Fig. 4. The top row demonstrates temperature transients in the system for the case when one of the bleed valves is stack open. This fault results in the increased fluid flow that speeds up chilldown dynamics. As a consequence, the temperature of the fluid in the pipe becomes lower than in nominal regime. The deviation of the flow temperature beyond low margin can be detected by several sensors.

Similar dynamic features are observed when a different bleed valve is stack open. The model predictions for the corresponding temperature time-series data are shown in the middle row.

The leak in the pipe also results in the increase of the flow rate and cooling upstream of the fault. The transient dynamics of the flow temperature detected by sensors in this case is shown in the bottom row of the Fig. 4. It follows very closely the dynamics observed in two previous cases making it difficult to identify of one of these three faults.

	t1	t2	t3	t4	t5	t6	t7	t8	t9	t10
f1	0	1	0	0	1	0	0	0	0	1
f2	1	0	1	1	0	1	1	1	0	0
f3	1	0	1	1	0	1	1	1	0	0
f4	0	1	0	0	1	0	0	0	1	0
f5	1	0	1	1	0	1	1	0	0	0
f6	0	1	0	0	1	0	0	0	0	0

Table 1. The fragment of the D-matrix build for two groups if faults using outcome of eight sensors. The two ambiguity groups are highlighted by pink and cyan. The predicted dependencies for two virtual sensors that can partially disambiguate the faults are highlighted in the last two columns by gray color.

6.3. Dependency matrix of the cryogenic chilldown

An efficient approach to the solution of this problem can be developed within D-matrix formalism (Sheppard & Simpson, 1996). In this approach each fault is projected on a binary sequence of the test results. In this sequence 1 corresponds to the dependency relation between faults and tests and 0 corresponds to no such relation. Overall, the directed graph corresponding to the logical relationships between the set of tests (results of the sensor measurements) and the set of diagnoses (faults) can be represented in a bit-wise D-matrix (Sheppard & Simpson, 1996).

An fragment of the D-matrix developed for the fault diagnostics in the cryogenic transfer line during chilldown is show in the Table **??**. There is a set of definitions used to optimized fault identification within D-matrix approach (Singh et al., 2009): (i) Some invalid test points are eliminated if these nodes have no contribution to fault diagnosis results; (ii) The undetectable faults which dont exist in a dependency matrix should be deleted; (iii) Some faults have same states combinations, these ambiguity faults should be combined.

These simple improvements were applied to the fragment of the D-matrix for the test set $\{t1, \ldots, t8\}$ presented in the Table **??**. Two ambiguity groups corresponding to the stack open (leaks) and stack closed (clogging) faults at different bleed valves are highlighted by cyan and pink colors.

It is well-known that the model-based frameworks can substantially enhance interaction of behavioral knowledge and diagnostic inference (Angeli & Chatzinikolaou, 2004). A more detailed discussion of the development of the on-line expert system for the IHM of cryogenic transfer will be given elsewhere. Here we provide two examples of how the model-based approach can be employed to disambiguate the faults within the ambiguity groups.

Firstly, model predictions can be used to analyze the performance of the virtual sensors and suggest appropriate modifications to the dependency matrix. A result of such analysis is shown in the Table **??**. The two virtual sensors proposed using simulations of the physics model are mass flow measurements at two specific locations. The corresponding dependencies are highlighted by gray color in the last two columns. It can be verified easily from the table that these two additional tests can help to resolve ambiguity in one of the groups while the second group of faults remains unresolved. We now show that these faults can be resolved at the evaluation stage using optimization tools within model-based framework.

7. EVALUATION

Once fault is identified to belong to one of the ambiguity groups the parameter space for subsequent fault analysis and evaluation is substantially reduced. At this stage a number of optimization tools can be employed to disambiguate and estimate the value of the fault.

In the numerical test described below three possible fault were identified: (i) valve cv1 stack open, (ii) valve cv2 stack open, and (iii) leak in one of the pipes. Their dynamic features (see Fig. 4 and faults f2, f3, f5 in the Table **??**) are very similar and additional analysis is required to disambiguate the fault. Three optimization tools were developed and tested for cryogenic chilldown model - unconstrained nonlinear optimization, the MCMC, and the direct search.

The unconstrained optimization is very efficient for the local search and fine tuning of the single parameter. In the case of search in the space of three parameters this algorithm tends to stack at multiple local minima. The MCMC algorithm with Metropolis-Hastings step was also dwelling on the local minima for prohibitively long time for on-line applications.

At the same time it was found that for three-dimensional parameter space the direct search algorithm is very efficient in locating the neighborhood of the global minimum and discerning between the faults within one ambiguity group. The results of application of this algorithm to the evaluation of the fault are shown in the Fig. 5.

The fault (valve cv2 stack open at 30%) was injected at 300 sec. It was almost immediately detected by one of the sensors and a short time later by two other sensors. We emphasize that only temperature sensors were able to detect the fault, while pressure sensors readings remained within the margins.

The identification procedure described in the previous section reduced the analysis of the fault root to three possible causes. To discern between the possible fault causes the following nonlinear curve fitting algorithm was employed. The model predictions for the temperature and pressure $\mathbf{F_n}(t_n, \mathbf{c_k})$ were fitted to the measured values of p_n and T_n on the time interval $t_0, ..., t_N$ (spanning from detection time to present time or the end of chilldown) at the sensor locations. The cost function was chosen in the form

$$S(\mathbf{c_k}) = \sum_{n=0}^{N} \left((F_{1,n} - p_n)^2 + (F_{2,n} - T_n)^2 \right)$$

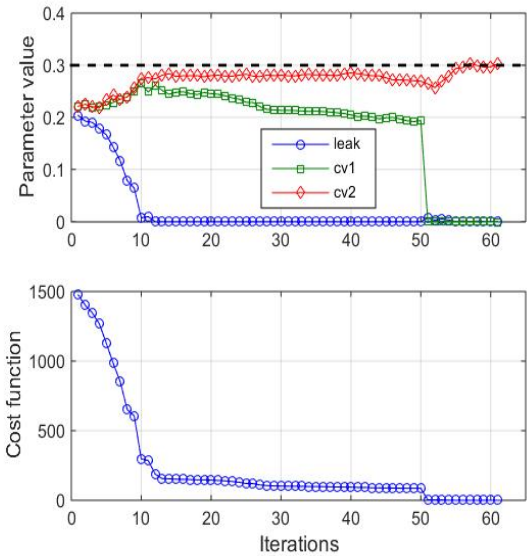

Figure 5. The results of discerning and evaluating faults within one ambiguity group.

where the $\mathbf{c_k}$ is the set of parameters of suspected faults.

By scanning through the parameter space it was possible to rule out two of the suspected faults and to estimate the value of the correctly identified remaining fault. In particular, it can be seen from the figure that the leak fault was ruled out after 10 iterations, and after 50 iterations it was possible to disambiguate between two suspected valve stack open faults. It can also be seen in the figure that the algorithm converges to the correct value of the fault in 60 iterations. Each iteration takes less than half a second of integration on a laptop.

The fault discerning and evaluation described above complete the example of application of the physics based approach to the integrated health management of cryogenic loading operation. It demonstrates that the physics based approach to the IHM of cryogenic systems may offer a number of significant extension and improvements of the IHM capabilities as compared to other techniques.

8. CONCLUSION

In conclusion we note that physics models develop within this project allow for very fast and time-accurate predictions of the pressure and temperature dynamics of cryogenic system during chilldown and loading operations. This capability opens a unique opportunity of developing model-based approach to the on-line health management of cryogenic systems.

We provided an example of application of the model-based approach to three basic steps of the integrated health management - fault detection, identification, and evaluation. We demonstrated that at every step the model-based approach can enhance and extend capabilities of the health management system. We emphasize that provided example refers to the chilldown operation, which is one of the most challenging regimes of loading from the point of view of model predictions and fault management.

We showed that model-based approach allows one to create and extend digital library of faults in cryogenic system that includes realistic dynamic features of the faults. It also allows one to create and optimize dependencies matrix between faults and sensors measurements that can be used for the fast on-line fault identification. We demonstrated that physics based analysis reveals several ambiguity groups for the faults in cryogenic system.

We developed a number of the model-based optimization tools that allows one to discern and evaluate faults within each ambiguity group. The development of these tools paves the way to a number of important applications of the model-based approach including machine learning of the system and flow parameters, optimization of the fault recovery strategies, loading regimes, and design of cryogenic systems. The results of the development of these applications will be discussed in details in our future work.

ACKNOWLEDGMENT

This work was supported by the Advanced Exploration Systems and Game Changing Development programs at NASA HQ.

NOMENCLATURE

u	velocity
T	temperature
p	pressure
e	specific energy
h	specific enthalpy
H	heat transfer coefficient
g	gravity
Re	Reynolds number
Fr	Froude number
Bo	Boiling number
t	time
Δt	time step
E	enhancement factor
A	cross-sectional area
V	volume of the control volume
f	friction factor
l	perimeter
z	coordinate along the pipe
x	mass fraction
y	height of the control volume
$\dot{m}$	mass flow rate
c	specific heat

Greek

α	gas void fraction
ρ	density
τ	wall shear stress
μ	viscosity

Subscript

g	gas
3	two-phase region
w	wall
a	ambient

REFERENCES

Angeli, C., & Chatzinikolaou, A. (2004). On-line fault detection techniques for technical systems: A survey [Journal Article]. *International Journal of Computer Science & Applications*, *1*(1), 12-30.

Brennan, J., Brentari, E., Smith, R., & Steward, W. (1966). *Cooldown of cryogenic transfer lines* [Experimental Report].

Chato, D. J. (2008). Cryogenic fluid transfer for exploration. *Cryogenics*, *48*(5-6), 206–209.

Hafiychuk, V., Foygel, M., Ponizovskaya-Devine, E., Smelyanskiy, V., Watson, M. D., Brown, B., & Goodrich, C. (2014). Moving-boundary model of cryogenic fuel loading, i: Two-phase flow in a pipe [Journal Article]. *Journal of Thermophysics and Heat Transfer*, 1-12.

Hafiychuk, V., Foygel, M., Ponizovskaya-Devine, E., Smelyanskiy, V., Watson, M. D., Brown, B., & Goodrich, C. (2015). Moving-boundary model of cryogenic fuel loading, ii: Theory versus experiments [Journal Article]. *Journal of Thermophysics and Heat Transfer*, 1-6.

Jensen, J., Jensen, J. M., & Tummescheit, H. (2002). Moving boundary models for dynamic simulations of two-phase flows. In *Proc. of the 2nd int. modelica conference.*

Johnson, R., Notardonato, W., Currin, K., & Orozco-Smith, E. (2012). Integrated ground operations demonstration units testing plans and status [Book Section]. In *Aiaa space 2012 conference & exposition.* American Institute of Aeronautics and Astronautics.

Kashani, A., Ponizhovskaya, E., Luchinsky, D., Smelyanskiy, V., Sass, J., Brown, B., & Patterson-Hine, A. (2014). Physics based model for online fault detection in autonomous cryogenic loading system [Journal Article]. *AIP Conference Proceedings*, *1573*(1), 1305-1310.

Luchinsky, D. G., Smelyanskiy, V. N., & Brown, B. (2014a). *Physics based model for cryogenic chilldown and loading. part i: Algorithm* (Technical Publication No. NASA/TP-2014-216659). NASA, ARC.

Luchinsky, D. G., Smelyanskiy, V. N., & Brown, B. (2014b). *Physics based model for cryogenic chilldown and loading. part ii: Verification and validation* (Technical Publication No. NASA/TP-2014-218298). NASA, ARC.

Prosperetti, A., & Tryggvason, G. (n.d.). *Computational methods for multiphase flow*. Cambridge University Press.

Sheppard, J. W., & Simpson, W. R. (1996). Improving the accuracy of diagnostics provided by fault dictionaries [Conference Proceedings]. In *Vlsi test symposium, 1996., proceedings of 14th* (p. 180-185).

Singh, S., Kodali, A., Choi, K., Pattipati, K. R., Namburu, S. M., Sean, S. C., ... Liu, Q. (2009). Dynamic multiple fault diagnosis: Mathematical formulations and solution techniques [Journal Article]. *Systems, Man and Cybernetics, Part A: Systems and Humans, IEEE Transactions on*, *39*(1), 160-176.

Thome, J. R. (2006). *Ch. 13, two-phase pressure drop*. (web book updated yearly).

Woldesemayat, M. A., & Ghajar, A. J. (2007). Comparison of void fraction correlations for different flow patterns in horizontal and upward inclined pipes. *International Journal of Multiphase Flow*, *33*(4), 347 - 370.

Zhang, W.-J., & Zhang, C.-L. (2006). A generalized moving-boundary model for transient simulation of dry-expansion evaporators under larger disturbances [Journal Article]. *International Journal of Refrigeration*, *29*(7), 1119-1127.

BIOGRAPHIES

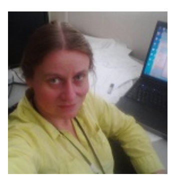

Ekaterina Ponizovskaya-Devine Dr. Ekaterina Ponizovskaya-Devine is a research scientist in SGT since 2009. Her current work is related to integrated health management and control of cryogenic propellant loading systems and two-phase cryogenic flow modeling. She obtained her PhD at Moscow institute of Physics and Technology in Physics, working on stochastic resonance in non-equilibrium electron-hole plasma. She was a post-doc in Spanish National Research Council, working in photonics, nanotechnology, negative index materials. In 2005 she had Visiting Scholar position at HP Lab working in nanotechnology. Her research interests are physics based models, two-phase flow, nanotechnology, physics model based fault diagnostics, optimization and control. .

Dmitry G. Luchinsky is a senior research scientist in MCT Inc. He obtained his MSc and PhD in physics in Moscow working on nonlinear optics of semiconductors. He is an author of more than 100 publications. He has been on a number of occasions a Royal Society Visiting Fellow and a NASA visiting scientist. He worked as a senior scientific researcher in VNII for Metrological Service (Moscow, Russia) and as a Senior Research Fellow in Lancaster University (Lancaster, UK). His research interests include nonlinear optics, stochastic and chaotic nonlinear dynamics, dynamical inference, fluid dynamics, ionic motion. His research is currently focused on theory and CFD of gas dynamics and cryogenic flows.

Michael Khasin Dr Michael Khasin is a Senior Researcher in SGT Inc., working at NASA Ames Research Center. He holds B.Sc. in Physics (Honors Program), 2001, M.Sc. in physics, 2003, and PhD in chemical physics, 2008, from the Hebrew University of Jerusalem. As a postdoctoral researcher at Michigan State University, Massachusetts Institute of Technology, and University of Michigan, Michael worked on the theory of non-equilibrium systems and their control and transport in disordered system. His research interests include applied physics, nonlinear and stochastic dynamics, large fluctuations and their control in non-equilibrium systems and efficient simulation of complex dynamics. He has been an invited speaker to many international and national conferences and workshops. Currently his research is focused on the theory of heat transfer, fluid dynamics, and fluid structure interaction.

Dŏgan A. Timuçin is a Research Scientist in the Intelligent Systems Division at NASA Ames Research Center. He holds B.S. (1989), M.S. (1991), and Ph.D. (1994) degrees in electrical engineering, and has been with NASA since 1995. His research interests are in the general areas of classical electrodynamics and optics, statistical physics, nonlinear dynamics, Bayesian inference, and numerical optimization.